Frenet-Artificial Potential Field Method for Vehicle Obstacle Avoidance Path Planning

2024 7th International Conference on Information Communication and Signal Processing (ICICSP) | 979-8-3503-5589-5/24/$31.00 ©2024 IEEE | DOI: 10.1109/ICICSP62589.2024.10809262

Qingdian Tang, Kai Liu, Jiaqin Wang, Qiang Gao
School of Electronics and Information Engineering
Beihang University
Beijing 100191, China
tqd030303@163.com
{liuk, wangjiaqin, gaoqiang}@buaa.edu.cn

Zhaobai Wen*
Information and Network Department
Wuhan Maritime Communication Research Institute
Wuhan 430079, China
179152992@qq.com
*Corresponding author

***Abstract*—Artificial potential field (APF) based vehicle obstacle avoidance path planning shows promise in improving traffic safety. However, traditional APF encounters challenges when applied in autonomous driving scenarios due to its inherent limitations and the realistic constraints of traffic dynamics. To solve the problem, this paper proposes the Frenet-artificial potential field (Frenet-APF) method. Firstly, to overcome traditional APF limitations, we introduce a regulatory factor into the repulsive potential field to handle unreachable target points issues, and constructs a heading-adjustable safe ellipse model to resolve local optimal issues. Secondly, for adaptation to multi-lane structured road, we construct a structured road repulsive potential field to meet route constraints. Thirdly, to enhance safety against dynamic obstacles, we design a virtual target point-guided lane change strategy into APF, enabling proactive lane change. Fourthly, for application in large curvature paths, we combine the improved APF with Frenet coordinates to simplify curve into straight scenarios. Finally, simulation results demonstrate that the proposed algorithm successfully generates an efficient, smooth and collision-free path in structured road scenarios with large curvature, multi-lanes and multi-dynamic obstacles.**

Keywords—vehicle path planning, obstacle avoidance, artificial potential field, Frenet coordinates

I. INTRODUCTION

Path planning is a critical task of automatic driving system, which can be divided into two steps from the macro and micro aspects: routing and motion planning [1]. Artificial potential field (APF) has been widely used in path planning for autonomous vehicles because of its simple calculation and real-time performance [2]. However, the traditional APF has limitations of local optimal and unreachable target points. Researchers have done a lot of work to solve these problems. For instance, Yuan [3] used correction factors and relative distances to correct the potential function. Li et al. [4] added the concepts of safe distance and time distance detection method into potential function. Luo et al. [5] proposed a virtual potential field detection circle model with adjustable radius to detect the minimum trap in advance.

Meanwhile, to enhance the performance of planned paths in terms of safety, efficiency and smoothness, researchers have implemented numerous improvements for APF. For instance, Hao et al. [6] employed a collision risk assessment mechanism to avoid unreasonable obstacle avoidance actions and reduce the length of planned paths. Li et al. [7] established the cost function with safety and smoothness as the evaluation index to improve the safety of the obstacle avoidance process and the smoothness of the generated path. Ji et al. [8] constructed a three-dimensional potential field and obtained a shorter and smoother local path.

However, besides addressing these limitations and improving performance, most studies fail to address the challenge of adapting APF to complex autonomous driving scenarios, particularly on large curvature roads. Therefore, this paper combines the improved APF with Frenet coordinates and proposes Frenet-artificial potential field (Frenet-APF) method to effectively apply it in scenarios with large curvature, multi-lanes and multi-dynamic obstacles.

This paper is structured as follows. Section II briefly introduces the traditional APF. Section III presents the the Frenet-APF method. Section IV shows simulation results. Section V concludes the paper.

II. TRADITIONAL APF

APF establishes a repulsive potential field around obstacles and an attractive potential field around the target point. Combining these potential fields into a compound field, the controlled vehicle navigates along the negative gradient of potential energy to discover a path that avoids collisions.

The mathematical expression of attractive potential energy $U_{att}(q)$, repulsive potential energy $U_{rep}(q)$ and resultant potential field $U(q)$ are as follows:

$$U_{att}(q) = \frac{1}{2}\eta_{att}\rho^2(q, q_g), \tag{1}$$

$$U_{rep}(q) = \begin{cases} \frac{\eta_{rep}}{2}\left(\frac{1}{\rho(q,q_o)} - \frac{1}{\rho_0}\right)^2, \rho(q,q_o) < \rho_0 \\ 0, \rho(q,q_o) \geq \rho_0, \end{cases} \tag{2}$$

$$U(q) = U_{att}(q) + \sum_{i=1}^{m} U_{rep,i}(q). \tag{3}$$

This work was supported by the National Key Research and Development Program of China under Grant No. 2021YFB1600503.

Authorized licensed use limited to: BEIHANG UNIVERSITY. Downloaded on May 15,2026 at 08:40:18 UTC from IEEE Xplore. Restrictions apply.

where η_{att} and η_{rep} are gain coefficients, $\rho(q,q_g)$ is the Euclidean distance between the current point q and the target point q_g, $\rho(q,q_o)$ is the Euclidean distance between q and the obstacle point q_o, ρ_0 is the maximum influence range of the repulsive potential field, and m is the number of obstacles.

Calculating the negative gradient of potential energy, the mathematical expression of attractive force $F_{att}(q)$, repulsive force $F_{rep}(q)$ and resultant force $F(q)$ are as follows:

$$F_{att}(q) = -\nabla U_{att}(q) = \eta_{att}(q, q_g), \tag{4}$$

$$F_{rep}(q) = \begin{cases} \eta_{rep}\left(\frac{1}{\rho(q,q_o)} - \frac{1}{\rho_0}\right)\frac{\nabla\rho(q,q_o)}{\rho(q,q_o)^2}, \rho(q,q_o) < \rho_0 \\ 0, \rho(q,q_o) \geq \rho_0, \end{cases} \tag{5}$$

$$F(q) = F_{att}(q) + \sum_{i=1}^{m} F_{rep,i}(q). \tag{6}$$

III. Frenet-APF Method

Based on the traditional APF, we make four improvements for APF, namely regulatory factor, heading adjustable safe ellipse model, structured road repulsive potential field model and virtual target point-guided lane change strategy, thereby modifying the potential field method and optimizing the computation process. Furthermore, we combine the improved APF with Frenet coordinates to generate path.

A. Regulatory Factor

When an obstacle is near the target point, placing the target within its influence range, the target ceases to be the global minimum of potential energy. Consequently, the attractive force exerted on the vehicle towards the target becomes zero, while the repulsive force remains a certain amount, thereby resulting in the issue of the target being unreachable.

To address this issue, a regulatory factor has been introduced into the repulsive potential field, which ensures that both the attractive and repulsive forces diminish to zero simultaneously. The mathematical expression of the improved repulsive potential field is

$$U_{rep}(q) = \begin{cases} \frac{\eta_{rep}}{2}\left(\frac{1}{\rho(q,q_o)} - \frac{1}{\rho_0}\right)^2 \rho(q,q_g)^n, \rho(q,q_o) < \rho_0 \\ 0, \rho(q,q_o) \geq \rho_0, \end{cases} \tag{7}$$

where n is the regulatory factor coefficient. The corresponding repulsive force function is

$$F_{rep}(q) = \begin{cases} F_{rep1}(q) + F_{rep2}(q), \rho(q,q_o) < \rho_0 \\ 0, \rho(q,q_o) \geq \rho_0, \end{cases} \tag{8}$$

$$F_{rep1}(q) = \eta_{rep}\left(\frac{1}{\rho(q,q_o)} - \frac{1}{\rho_0}\right)\frac{\rho(q,q_g)^n}{\rho(q,q_o)^2}\nabla\rho(q,q_o), \tag{9}$$

$$F_{rep2}(q) = \frac{n\eta_{rep}}{2}\left(\frac{1}{\rho(q,q_o)} - \frac{1}{\rho_0}\right)^2 \rho(q,q_g)^{n-1}\nabla\rho(q,q_g). \tag{10}$$

Comparison of the algorithms before and after improvement is illustrated in Fig. 1, demonstrating that the enhanced algorithm successfully reaches the target point.

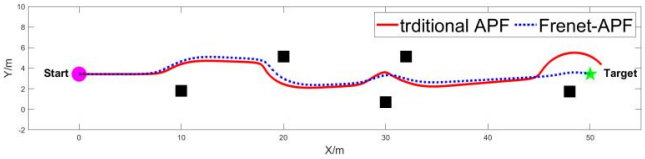


Fig. 1. Comparison diagram before and after introducing regulatory factor.

B. Heading Adjustable Safe Ellipse Model

The traditional repulsive influence range forms an isotropic circle. If the maximum influence range ρ_0 is too large, it can unnecessarily elongate the horizontal planned path. Conversely, if ρ_0 is too small, the longitudinal safety distance may be inadequate, potentially leading to collisions during obstacle avoidance. Thus, the efficiency and safety of the circular repulsive potential field are in conflict.

Therefore, we introduce the heading-adjustable safe ellipse model to adjust the ellipse longitudinal and horizontal axes to match the vehicle length and width by considering variations of vehicle size. To ensure safety during obstacle avoidance, a specific safety margin is maintained along the ellipse's longitudinal axis. The mathematical expression for the elliptical influence range is

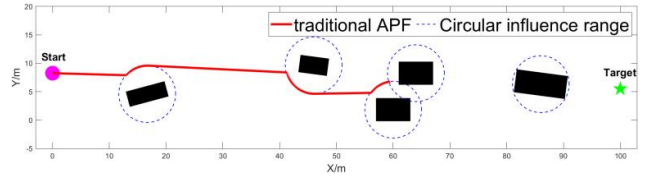
$$\rho(q,q_o) = \sqrt{\frac{(x^{'} - x_0)^2}{(\frac{kL}{2} + v_r t)^2} + \frac{(y^{'} - y_0)^2}{(\frac{kW}{2})}} \leq 1, \tag{11}$$

where L and W are vehicle length and width, v_r is the relative speed of the controlled and obstacle vehicle, t is the braking time, and k is the elliptic gain coefficient.

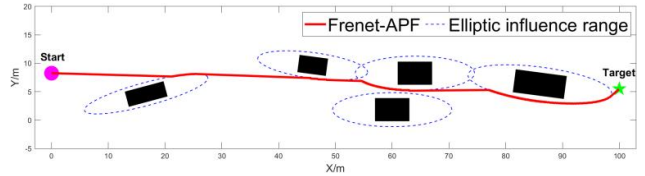
Taking into account the heading angle of the vehicle, a rotation transformation of the coordinates is required:

$$\begin{bmatrix} x^{'} \\ y^{'} \end{bmatrix} = \begin{bmatrix} \cos\theta & -\sin\theta \\ \sin\theta & \cos\theta \end{bmatrix}\begin{bmatrix} x \\ y \end{bmatrix}, \tag{12}$$

where (x,y) is the original coordinate, (x',y') is the coordinate after rotation, and θ is the heading angle.



(a). Circular repulsive force potential field.



(b). Elliptical repulsive force potential field.

Fig. 2. Comparison diagram before and after introducing ellipse model.

Authorized licensed use limited to: BEIHANG UNIVERSITY. Downloaded on May 15,2026 at 08:40:18 UTC from IEEE Xplore. Restrictions apply.

Five obstacles of varying sizes and orientations are randomly positioned in the scene to evaluate the performance of both the circular and elliptical repulsive potential fields. The corresponding results is illustrated in Fig. 2.

Comparing the elliptical repulsive potential field with the circular one, the planned path successfully avoids local optimal. This is because the elliptical model reduces the horizontal influence range, mitigating the risk of encountering local minima due to overlapping influence zones of adjacent obstacles during longitudinal movement.

C. Structured Road Repulsive Potential Field Model

In structured road environments, there are two fundamental types of road markings, including boundary lines and lane lines. Each type imposes specific constraints on vehicle movement:

1) Boundary line: Vehicles must drive within the boundary line and cannot cross it.

2) Lane line: Vehicles are required to stay as close as possible to the lane center, with the option to cross lane lines when necessary to avoid obstacles.

To meet these constraints, we incorporate an additional structured road repulsive potential field into the original potential field, including the boundary line repulsive potential field (BPF) and the lane line repulsive potential field (LPF).

The structured road repulsive potential field of a five-lane road is illustrated in Fig. 3.

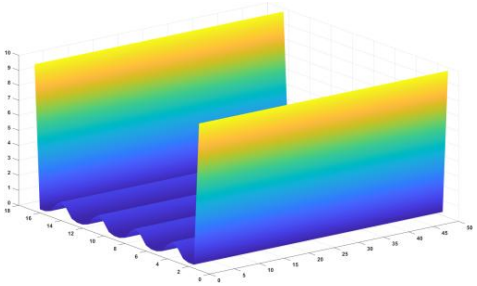


Fig. 3. Road repulsive potential field.

The LPF can be modeled using a sine function, where the trough aligns with the lane center and the crest corresponds to the lane line. The mathematical expression is

$$U_{LPF}(q) = \eta_L[\cos\frac{2\pi}{W_L}\rho(q,q_L)+1], \tag{13}$$

where, $\rho(q,q_L)$ is the vertical distance from the current point to the lane line, η_L is the LPF gain coefficient, and W_L is the LPF influence region width.

BPF can be modeled using a hook function. The mathematical expression is

$$U_{BPF}(\mathrm{q}) = \eta_B[\rho(q,q_B)+\frac{k_b}{\rho(q,q_B)\text{-}S}+k_d], \tag{14}$$

where, $\rho(q,q_B)$ is the vertical distance from the current point to the boundary line, η_B is the BPF potential field gain coefficient, S is the safety width to consider the vehicle width, W_B is the BPF influence region width, k_b and k_d are smooth adjustment coefficients to ensure continuity of derivatives and the original functions at the junction between LPF and BPF.

After calculation, the value of k_b and k_d are

$$\begin{cases} k_b = {W_B}^2 \\ k_d = 2W_B - S. \end{cases} \tag{15}$$

Testing a scenario with two lanes and three obstacles, Fig. 4 compares the algorithms before and after introducing the structured road repulsive potential field. It demonstrates that the improved planned path avoids crossing the boundary lines and can adhere closely to the lane center, satisfying the lane routing constraints effectively.

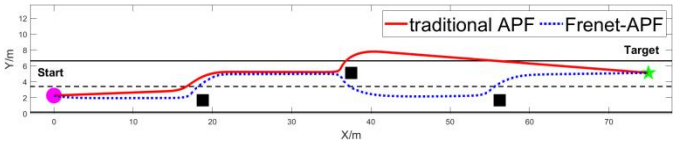
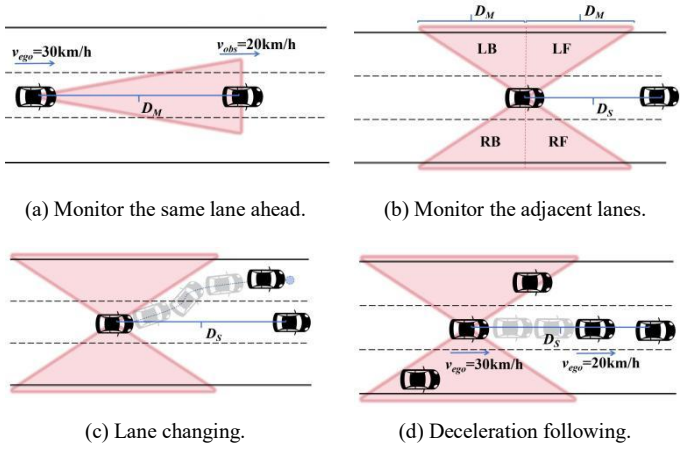


Fig. 4. Comparison diagram before and after introducing road potential field.

D. Virtual Target Point-Guided Lane Change Strategy

We propose the virtual target point-guided lane change strategy to enhance the performance when encountering dynamic obstacles. The core concept involves placing a temporary virtual target point in the adjacent lane, guiding the controlled vehicle to preemptively avoid the dynamic obstacle vehicle, ensuring the safety of the obstacle avoidance process. The key processes of this strategy are shown in Fig. 5, and the strategy unfolds as follows:



(a) Monitor the same lane ahead. (b) Monitor the adjacent lanes.

(c) Lane changing. (d) Deceleration following.

Fig. 5. Key processes of virtual target point-guided lane change strategy.

1) Monitor the same lane ahead status: If the speed of the obstacle vehicle within the monitored distance D_M ahead in the same lane is slower than the controlled one or moving in the opposite direction, as illustrated in Fig. 5(a), the gap between them continues to decrease, posing a collision risk.

2) Calculate the safety warning distance: As the gap narrows, the timing for obstacle avoidance is adjusted based on the relative velocity v_r to improve safety. Thus, the safety warning distance D_S is directly proportional to v_r. A higher v_r

Authorized licensed use limited to: BEIHANG UNIVERSITY. Downloaded on May 15,2026 at 08:40:18 UTC from IEEE Xplore. Restrictions apply.

leads to a smaller D_S, emphasizing the need for more urgent obstacle avoidance.

3) Monitor the adjacent lane status: Upon reaching the safety warning distance, it becomes essential to monitor the conditions of the left and right adjacent lanes to assess their suitability for lane change. The monitoring range can be divided into four segments: left front (LF), left back (LB), right front (RF) and right back (RB), as illustrated in Fig. 5(b). For instance, regarding the left adjacent lane, Table I outlines the conditions that satisfy the lane-change criteria.

TABLE I. COMBINATION OF LANE CHANGING CONDITIONS

Lane conditions		**The reason for allowing lane changes**
LF	***LB***	
Car-free	Car-free	There are no cars
Car-free	Slow-moving cars	The distance between the obstacle and controlled cars is getting larger
Fast-moving cars	Car-free	
Fast-moving cars	Slow-moving cars	

4) Change lanes to avoid obstacles or slow down to follow: If both the left and right lanes meet the lane-changing conditions, a lane is randomly selected to set a virtual target point, as illustrated in Fig. 5(c). In cases where neither adjacent lane meets this conditions, the speed of the vehicle will be reduced to the same speed as that of the preceding vehicle, and it will move with the preceding vehicle, as illustrated in Fig. 5(d).

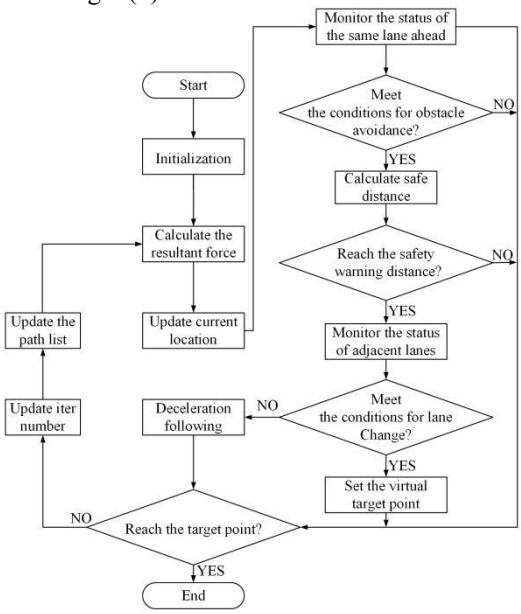


Fig. 6. Flowchart of APF integrated with lane change strategy.

This strategy is incorporates into the improved APF, and the algorithm flow is illustrated in Fig. 6.

E. Frenet Coordinate System

The Frenet coordinate system is widely utilized in path planning tasks [9]. Unlike the Cartesian coordinate system, Frenet coordinate system decouples the two-dimensional position vector into two independent one-dimensional components of longitudinal and lateral displacement, thereby simplifying the path planning process.

To address the challenge of obstacle avoidance with large curvature roads, the Frenet-APF method combines the improved APF with the Frenet coordinates. The specific approach is as follows. Firstly, the absolute positions of the controlled vehicle, obstacle vehicles, and lane routes in Cartesian coordinates are converted into relative positions using Frenet coordinates based on the Frenet reference line. Secondly, utilizing the position information in Frenet, the improved APF generates a local path. Finally, the path position information of Frenet is converted back to Cartesian.

Meanwhile, we use the global path generated by A* algorithm as the reference line of Frenet coordinate system, which realizes the organic combination of routing and motion planning. The Frenet-APF framework is illustrated in Fig. 7.

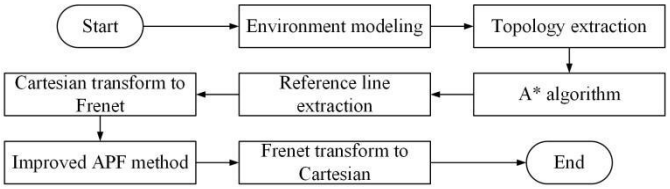


Fig. 7. Frenet-APF framework.

IV. SIMULATION RESULTS

A. Performance Comparison of Different Methods

In order to prove the performance superiority of the proposed algorithm, this paper constructs a test scenario to compare rapidly exploring random tree (RRT), which is a widely used sample-based path planning method, and traditional APF with Frenet-APF. The scenario is 50 meters long and 10 meters wide, with seven randomly placed obstacles of different sizes and orientations. Simulation results are illustrated in Fig. 8, and a detailed performance comparison is presented in Table II.

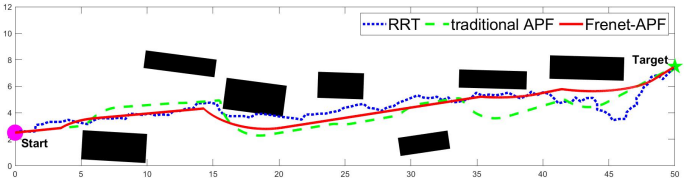


Fig. 8. Comparison results among different methods.

TABLE II. COMPARISON OF RELATED PERFORMANCE INDICATORS

Algorithm	**Iteration step**	**Simulation time/s**	**Path length/m**
RRT	0.5	1.3849	58.0393
Traditional APF	0.5	0.2092	53.5280
Frenet-APF	0.5	0.4919	50.6507

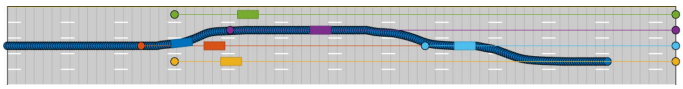
As shown in Fig. 8, compared with RRT and traditional APF, the path generated by Frenet-APF is smoother and maintains a greater longitudinal safety distance during obstacle avoidance, demonstrating superior stability and security. Meanwhile, Table II illustrates that the Frenet-APF method can

Authorized licensed use limited to: BEIHANG UNIVERSITY. Downloaded on May 15,2026 at 08:40:18 UTC from IEEE Xplore. Restrictions apply.

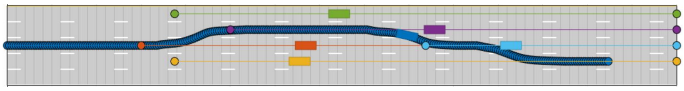
obtain the shortest path length under the same iteration step, and the simulation time is quite short, demonstrating superior efficiency and real-time performance.

B. *Performance Comparison in Different Scenarios*

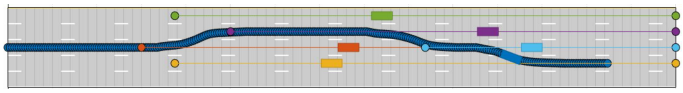
The MATLAB Automated Driving Toolbox is employed as the simulation tool in this paper to create two traffic scenarios, including straight and curved structured roads. The test results illustrate the adaptability of the Frenet-APF method to multi-lane, dynamic obstacles and large curvature environments, as shown in Fig. 9 and Fig. 10, respectively.



(a) First lane change.

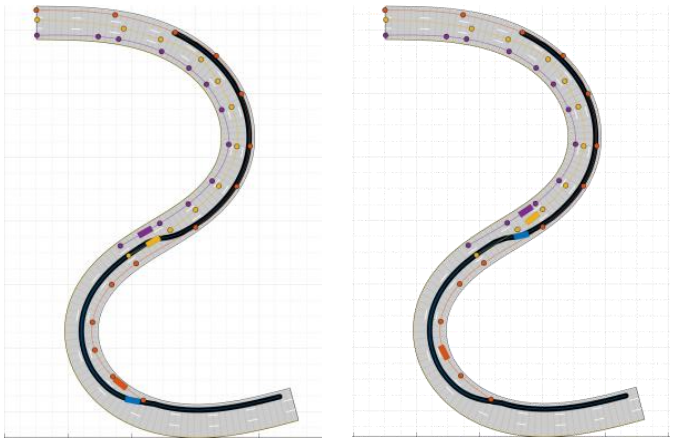


(b) Second lane change.



(c) Third lane change.

Fig. 9. Straight road simulation test results.



(a) First lane change.

(b) Second lane change.

Fig. 10. S-shaped road simulation test results.

Fig. 9 shows that employing the virtual target point enables the controlled vehicle successfully realize three flexible proactive lane changes between multiple lanes when there are dynamic obstacles, verifying the algorithm adaptability of multi-lanes and multi-dynamic obstacles. Fig. 10 shows that the controlled vehicle generates a smooth and collision-free planned path under S-shaped road, validating the algorithm adaptability of large curvature paths.

V. CONCLUSION

This paper proposes the Frenet-APF method, which combines the improved APF with Frenet coordinates. The proposed method address the unreachable target points and local optimal issue, while meeting the realistic constraints of traffic dynamics including large curvature paths, multi-lane structured roads and dynamic obstacles. Simulation results show that compared with RRT and traditional APF, this method has advantages in path efficiency, smoothness, real-time and safety, and can generate smooth, efficient and collision-free local paths in various automatic driving scenarios. The specific conclusions are as follows.

(1) Overcome the limitations of traditional APF: Firstly, we introduce a regulatory factor with a coordinating force to ensure the target point becomes the global minimum to resolve the unreachable target point issues. Secondly, we construct a heading-adjustable safe ellipse model, which effectively prevents the overlap of the repulsive potential field influence ranges to overcome local optimal issues.

(2) Meet the realistic constraints of traffic dynamics: Firstly, we introduce a structured road repulsive potential field to ensure vehicles adhere to lane boundaries and remain centered within lanes, facilitating flexible and stable lane changes for multi-lane structured roads. Secondly, we integrate a virtual target point-guided lane change strategy with APF to enable early detection of dynamic obstacles and proactively lane change in order to avoid dynamic obstacles. Thirdly, we combine APF with Frenet coordinates to decouples absolute two-dimensional coordinates into one-dimensional relative position information, transforming curved road planning into straight road equivalents.

REFERENCES

[1] X. Zhou, X. Yu, Y. Zhang, Y. Luo, and X. Peng, “Trajectory Planning and Tracking Strategy Applied to an Unmanned Ground Vehicle in the Presence of Obstacles,” IEEE Transactions on Automation Science and Engineering, vol. 18, no. 4, pp. 1575–1589, Oct. 2021.

[2] J. Pan, Y. Jiang, and J. Mao, “Vehicle Local Path Planning Based on Artificial Potential Field Method,” in 2024 7th International Conference on Advanced Algorithms and Control Engineering (ICAACE),Shanghai, China, Mar. 2024, pp. 1446–1449.

[3] X. Yuan, “Research on the Limitations of UAV Path Planning Based on Artificial Potential Field Method,” in 2022 9th International Forum on Electrical Engineering and Automation (IFEEA), Zhuhai, China, Nov. 2022, pp. 619–622.

[4] Y. Li, B. Tian, Y. Yang, and C. Li, “Path Planning of Robot Based on Artificial Potential Field Method,” in 2022 IEEE 6th Information Technology and Mechatronics Engineering Conference (ITOEC), Chongqing, China, Mar. 2022, pp. 91–94.

[5] J. Luo, Z.-X. Wang, and K.-L. Pan, “Reliable Path Planning Algorithm Based on Improved Artificial Potential Field Method,” IEEE Access, vol. 10, pp. 108276–108284, Oct. 2022.

[6] G. Hao, Q. Lv, Z. Huang, H. Zhao, and W. Chen, “UAV Path Planning Based on Improved Artificial Potential Field Method,” Aerospace, vol. 10, no. 6, pp. 562, Jun. 2023.

[7] H. Li, W. Liu, C. Yang, W. Wang, T. Qie, and C. Xiang, “An Optimization-Based Path Planning Approach for Autonomous Vehicles Using the DynEFWA-Artificial Potential Field,” IEEE Transactions on Intelligent Vehicles, vol. 7, no. 2, pp. 263–272, Jun. 2022.

[8] Y. Ji, L. Ni, C. Zhao, C. Lei, Y. Du, and W. Wang, “TriPField: A 3D Potential Field Model and Its Applications to Local Path Planning of Autonomous Vehicles,” IEEE Transactions on Intelligent Transportation Systems, vol. 24, no. 3, pp. 3541–3554, Mar. 2023.

[9] M. Werling, J. Ziegler, S. Kammel, and S. Thrun, “Optimal Trajectory Generation for Dynamic Street Scenarios in a Frenét Frame,” in 2010 IEEE International Conference on Robotics and Automation, Anchorage, AK, USA, May. 2010, pp. 987–993.

Authorized licensed use limited to: BEIHANG UNIVERSITY. Downloaded on May 15,2026 at 08:40:18 UTC from IEEE Xplore. Restrictions apply.